Preparation of peracetic acid from hydrogen peroxide, part II: Kinetics for spontaneous decomposition of peracetic acid in the liquid phase

Xuebing Zhao [a,*], Keke Cheng [b], Junbin Hao [b], Dehua Liu [a,**]

[a] *Institute of Applied Chemistry, Department of Chemical Engineering, Tsinghua University, Beijing 100084, China*
[b] *Institute of Nuclear and New Energy Technology, Tsinghua University, Beijing 100084, China*

Abstract

A homogeneous kinetic model was developed for describing the synthesis, hydrolysis and spontaneous decomposition of peracetic acid (PAA) in the liquid phase under an acid condition. It was found that the chelant (diethylenetriaminepenta acetic acid, DTPA) was not so effective for reduction of PAA decomposition in a strong acid solution as it in a neutral or alkaline aqueous solution. The expressions for calculating the rate constants of PAA synthesis and hydrolysis obtained in our previous work were still appropriate at a high temperature. The spontaneous decomposition of PAA under an acid condition was an observed second-order reaction with respect to PAA concentration. The observed rate constant was a relatively complicated function of temperature and H^+ concentration. Addition of sulfuric acid could significantly decrease the PAA decomposition. The reaction mechanism was investigated. It was proved that the rate-determining step for the spontaneous decomposition of PAA was the reaction between PAA molecule and a proton-activated carbonyl intermediary. The application of the kinetic model was further discussed.
© 2008 Elsevier B.V. All rights reserved.

Keywords: Peracetic acid; Hydrogen peroxide; Kinetics; Spontaneous decomposition; Reaction mechanism

1. Introduction

Peracetic acid (PAA) is the mono-acetyl derivative of hydrogen peroxide. It is a strong oxidant with a reduction potential of 1.06 V, which is similar to that of traditional bleaching agent, chlorine dioxide [1]. It has been applied in disinfection [2,3], bleaching of textiles and pulps [4–7], epoxidation of olefins [8,9] and so on. PAA is usually prepared by mixing acetic acid (AA) and hydrogen peroxide (HP) with sulfuric acid (SA) as a catalyst [10]. This reaction is reversible, which proceeds to an equilibrium mixture of reactants and products, as shown in Eq. (1).

$$CH_3COOH + H_2O_2 \underset{H^+}{\overset{}{\rightleftharpoons}} CH_3COOOH + H_2O \qquad (1)$$

We investigated the kinetics for PAA synthesis and hydrolysis in our previous work and found that both of the forward and reverse reactions were first-order with respect to PAA concentration and H^+ concentration at a temperature below 323 K [11]. However, the spontaneous decomposition of PAA at a higher temperature will become too significant to be negligible. It has been reported [12–14] that PAA in solution may be consumed in the following three reactions:
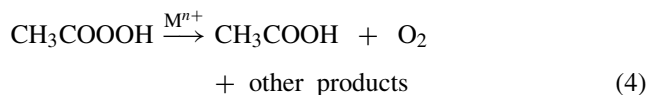
1. The hydrolysis:

$$CH_3COOOH + H_2O \rightarrow CH_3COOH + H_2O_2 \qquad (2)$$

2. The spontaneous decomposition:

$$2CH_3COOOH \rightarrow 2CH_3COOH + O_2 \qquad (3)$$

3. The transition metal ions catalyzed decomposition:

$$CH_3COOOH \overset{M^{n+}}{\longrightarrow} CH_3COOH + O_2 \\ + \text{ other products} \qquad (4)$$

* Corresponding author. Tel.: +86 10 62782654; fax: +86 10 62785475.
** Corresponding author. Tel.: +86 10 62792128; fax: +86 10 62785475.
E-mail addresses: zhaoxb04@mails.tsinghua.edu.cn (X. Zhao),
dhliu@tsinghua.edu.cn (D. Liu).

Nomenclature

a	activity
A, B, C and D	components names, denoting acetic acid, hydrogen peroxide, peracetic acid and water, respectively
AA	acetic acid
C_{X0}	initial concentrations of species X (mol L^{-1})
C_X	concentration of species X (mol L^{-1})
C_{Xe}	equilibrium concentration of species X (mol L^{-1})
$\Delta_r G_m^0$	standard Gibbs energy change of molar reaction (kJ mol^{-1})
$\Delta_f G_m^0$	standard molar formation Gibbs energy (kJ mol^{-1})
HP	hydrogen peroxide
I	ionic strength
k_1	intrinsic rate constant of peracetic acid synthesis (L mol^{-2} h^{-2})
k_2	intrinsic rate constant of peracetic acid hydrolysis (L mol^{-2} h^{-2})
k_{1obs}	observed rate constant of peracetic acid synthesis (L mol^{-1} h^{-1})
k_{2obs}	observed rate constant of peracetic acid hydrolysis (L mol^{-1} h^{-1})
k_{3obs}	observed rate constant of spontaneous decomposition of peracetic acid (L mol^{-1} h^{-1})
K	thermodynamic equilibrium constant
$K_{a,AcH}$	thermodynamic dissociation constant of acetic acid
K_C	concentration equilibrium constant
$K_{C,AcH}$	concentration dissociation constant of acetic acid
PAA	peracetic acid
SA	sulfuric acid
T	temperature (K)

Greek symbols

γ	activity coefficient
δ	difference of calculated datum and experimental datum (%)

Subscripts

0	initial state
e	equilibrium state

Koubek studied the spontaneous decomposition of PAA in a pH range of 5.9–10.2. He found that the dependence of the kinetics on the total PAA concentration is second-order. The reaction rate at 25 °C reached a maximum at pH 8.2, which was equal to the pK_a of PAA [15]. Koubek proposed a kinetic model for spontaneous decomposition of PAA as follows:

pH ≤ 7.5

$$\frac{-d[CH_3CO_3H]_t}{dt} = k_{obs}[CH_3CO_3H]_t^2$$
$$= \frac{k_a[CH_3CO_3H]_t^2}{[H^+]} \qquad (5)$$

pH ≥ 9.0

$$\frac{-d[CH_3CO_3H]_t}{dt} = k_{obs}[CH_3CO_3H]_t^2$$
$$= k_a[H^+][CH_3CO_3H]_t^2 \qquad (6)$$

It can be known from Eq. (5) that increasing H$^+$ concentration will result in decrease of PAA decomposition. However, the kinetic model did not mention the hydrolysis of PAA. Actually, we have found that in the preparation of PAA, the hydrolysis of PAA was much more important than its spontaneous decomposition at a low temperature. Yuan et al. [14] improved the kinetic equations with consideration of PAA hydrolysis, as shown in the following expression:

$$-\frac{d[CH_3CO_3H]_t}{dt}$$
$$= 9.21 \times 10^{13} \ \exp\left(\frac{-11338.71}{T}\right) \frac{2[H^+]/K_a[CH_3CO_3H]_t^2}{(1 + [H^+]/K_a)^2}$$
$$+ \left\{ 2.32 \times 10^8 \ \exp\left(\frac{-7488.68}{T}\right) \frac{K_a}{K_a + [H^+]} + 1.19 \times 10^9 \right.$$
$$\left. \times \exp\left(\frac{-5903.40}{T}\right) \frac{[H^+]}{K_a + [H^+]} \right\}[OH^-][CH_3CO_3H]_t \qquad (7)$$

Nevertheless, these models could not accurately predict our experimental data obtained in the preparation of PAA at a temperature above 323 K. We found that the model-calculated data were much smaller than the corresponding experimental data. It may be because that the reaction under a strong acid condition follows a different reaction mechanism, which results in a different kinetic behavior of PAA decomposition. According to Koubek [12] and Yuan et al. [13], the spontaneous decomposition of PAA in the pH range of 5.5–10.2 follows a mechanism as shown in Scheme 1.

However, in the preparation of PAA, the H$^+$ concentration in the system is usually more than 0.1 mol L^{-1}. It indicates that PAA is present as molecular form and no peraetic anion is found in the reaction solution. Therefore, the above mechanism and kinetic models are not appropriate any more for our reaction system. The objective of this article is thus to investigate the
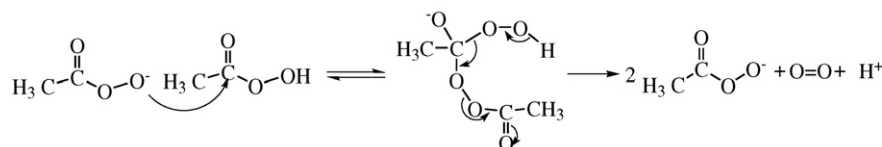
Scheme 1. The mechanism of spontaneous decomposition of PAA in the pH range of 5.5–10.2.

kinetics for the spontaneous decomposition of PAA in the liquid phase and discuss the reaction mechanism, which can serve as a step for further optimization of PAA preparation and some other related studies.

2. Experimental

2.1. Materials and experiment

All the chemicals used in the experiments, including anhydrous acetic acid, 30% hydrogen peroxide, potassium permanganate, potassium iodide, sodium thiosulfate, sulfuric acid and so on, were analytically pure and purchased locally. The contents of Fe^{3+} and Cu^{2+} in the reaction system were less than 0.5 and 0.2 ppm, respectively. Other metal ion contents were below the detection limit of the atomic absorption spectroscopic analysis method. Deionized water was used in all the experiments.

In the preparation of PAA, 30.0 mL AA and certain amount of 98% SA were put in each 50 mL clean ground-glass stoppered flask until SA concentrations in the system were 0.00, 0.0125, 0.0626, 0.1250 and 0.3125 mol L^{-1}, respectively. Then 15.0 mL HP solution was added to each flask and mixed homogeneously. The system was kept at a constant temperature in a water bath. Samples were taken and quickly analyzed at a certain reaction time. No chelant was used in the experiment, because our pre-experiment indicated that the chelant gave no contribution to decrease the decomposition of PAA in our system (see Fig. 1 in part 3.1).

2.2. Analytical method

The concentrations of PAA and HP were determined in accordance with the Chinese Standard GB/T 19108-2003. The principle could be summarized as that HP was first titrated with potassium permanganate and then PAA was determined iodometrically. Each of the experimental data was the average result of at least duplicate tests.

The kinetic constants were fitted according to the experimental data by a simplex optimization method using Matlab 6.5 software to minimize the objective function ($f_{objective}$), which was the quadratic sum of the difference between calculated data ($f(x_i)$) and experimental data (y_i), as shown in the following expression:

$$f_{objective} = \sum_{i=1}^{n} \delta_i^2 = \sum_{i=1}^{n} [f(x_i) - y_i]^2 \qquad (8)$$

The four-order Runge–Kutta method was used for the numerical solution of differential equations.

3. Results and discussion

3.1. Effect of diethylenetriaminepenta acetic acid (DTPA) on decomposition of PAA

Chelating agents are often added to hinder reactions between peroxide and metal ions. DTPA is one of the most effective chelant for reducing the free metal ions in the liquid. However,
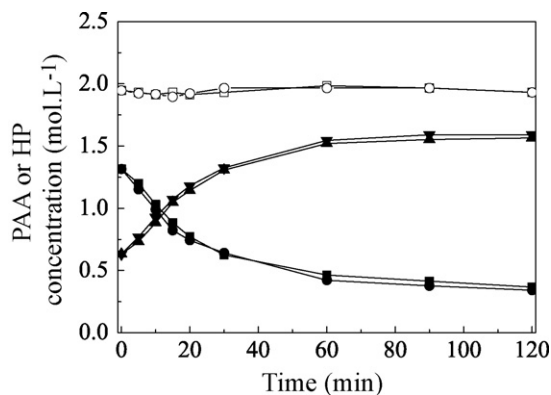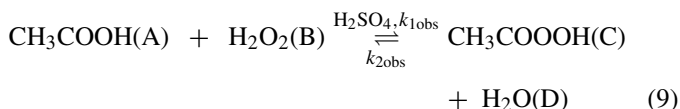

Fig. 1. Effect of DTPA on PAA and HP concentration at 333 K (the solution was non-equilibrium mixture of PAA, AA, HP and water; (■) PAA, 0.5 g L^{-1} DTPA; (●) PAA, no DTPA; (▲) HP, 0.5 g L^{-1} DTPA; (▼) HP, no DTPA; (□) PAA + HP, 0.5 g L^{-1} DTPA; (○) PAA + HP, no DTPA).

our experimental data (see Fig. 1) indicated that the consumption of PAA was not found decreased by addition of DTPA. Oppositely, it can be observed that DTPA could somewhat lead to an increase of PAA hydrolysis to form HP, but the concentration of total peroxides (PAA + HP) were not different. According to Yuan et al. [13,16], DTPA had a positive effect on reduction of PAA decomposition in the pH range of 5.5–7.5. It seemed that DTPA was not so effective in such a strong acid solution as it in a neutral or alkaline solution. It was probably because that large amount of AA could play as a chelant in our reaction system. On the other hand, DTPA also could be oxidized by PAA [16] which could lead to an additional consumption of PAA and make the reaction system more complicated. Therefore, no chelant was used in our kinetic study, and the metal ion-catalyzed decomposition of PAA and HP could be negligible.

3.2. Development of kinetic model

The thermal decomposition of HP in the liquid phase is not easily reached because the energy for break of O–O bond is relatively high ($\sim$51 kcal mol^{-1}) and homolysis of HP cannot happen unless it is heated above a critical temperature of 120 °C [17]. Therefore, the decomposition of HP in our system can be negligible. Actually, our experimental data also demonstrated that no obvious decomposition of HP was observed at 358 K, as shown in Fig. 2. It also indicated that the metal ion-catalyzed decomposition of HP could be negligible.

On the other hand, the homolysis of PAA can lead to a formation of radical species that can further induce PAA decomposition, but the activation energy of this decomposition is high and not readily reached in aqueous solutions [17]. Therefore, the reactions in the system mainly consist of the following types:
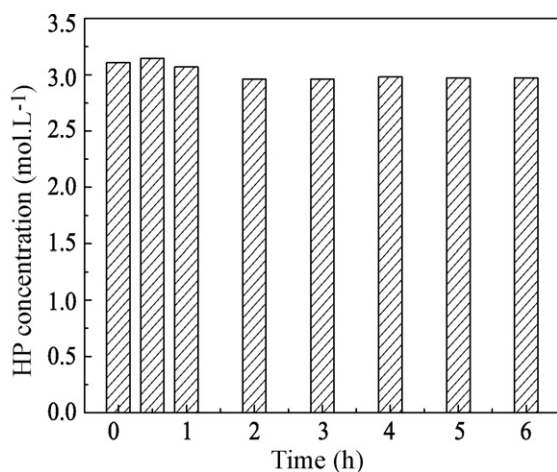
$$CH_3COOH(A) + H_2O_2(B) \underset{k_{2obs}}{\overset{H_2SO_4,k_{1obs}}{\rightleftharpoons}} CH_3COOOH(C)$$

$$+ H_2O(D) \qquad (9)$$

$$2CH_3COOOH \overset{k_{3obs}}{\longrightarrow} 2CH_3COOH + O_2 \qquad (10)$$

Fig. 2. HP concentrations without DTPA in the solution at 358 K.

where k_{1obs}, k_{2obs} and k_{3obs} are corresponding observed rate constants. An observed homogenous kinetic model thus can be developed as follows:

$$\frac{dC_B}{dt} = k_{2obs}C_CC_D - k_{1obs}C_AC_B \tag{11}$$

$$\frac{dC_C}{dt} = k_{1obs}C_AC_B - k_{2obs}C_CC_D - k_{3obs}C_C^2 \tag{12}$$

According to mass balance, the concentration of AA and water can be expressed as: $C_A = C_{A0} + C_{C0} - C_C$, $C_D = C_{D0} + C_{B0} - C_B$, where C_{X0} is the initial concentration of species X. The kinetic model thus can be written as:

$$\frac{dC_B}{dt} = k_{2obs}C_C(C_{D0} + C_{B0} - C_B)$$
$$- k_{1obs}(C_{A0} + C_{C0} - C_C)C_B \tag{13}$$

$$\frac{dC_C}{dt} = k_{1obs}(C_{A0} + C_{C0} - C_C)C_B$$
$$- k_{2obs}C_C(C_{D0} + C_{B0} - C_B) - k_{3obs}C_C^2 \tag{14}$$

According to our previous work, k_{1obs} and k_{2obs} had a linear relation with H^+ concentration ($[H^+]$) as $k_{1obs} = k_1[H^+]$ and $k_{2obs} = k_2[H^+]$, respectively, where k_1 and k_2 are intrinsic rate constants for the forward and reverse reactions [11]. We presume that k_{3obs} also is a function of $[H^+]$ and temperature (T)

that can be written as $k_{3obs} = f([H^+], T)$. Determination of the exact expression is also one of the objectives of this work.

In the system, H^+ mainly comes from two parts, dissociation of SA and AA:

$$[H^+] = [H^+]_{AcH} + [H^+]_{H_2SO_4} \tag{15}$$

The dissociation of AA is controlled by the equilibrium:

$$CH_3COOH \leftrightarrow CH_3COO^- + H^+ \tag{16}$$

The thermodynamic dissociation constant ($K_{a,AcH}$) and concentration dissociation constant ($K_{C,AcH}$) of AA can be related by the following expression:

$$K_{a,AcH} = \frac{a_{CH_3COO^-}a_{H^+}}{a_{CH_3COOH}} = \frac{\gamma_{CH_3COO^-}\gamma_{H^+}}{\gamma_{CH_3COOH}}K_{C,AcH} \tag{17}$$

where a and γ are activity and activity coefficient, respectively, with their relation of $a = \gamma C$. The activity coefficient γ can be calculated by Davies' formula:

$$\ln\gamma = -1.171|z_+z_-|\left[\frac{\sqrt{\{I\}}}{1 + \sqrt{\{I\}}} - 0.30\{I\}\right] \tag{18}$$

where $\{I\}$ denotes the value of ionic strength I. In our models, I was calculated approximately from molar concentration of species and degree of dissociation of AA (α):

$$I = \frac{1}{2}(b_{H^+} + b_{CH_3COO^-} + 4b_{SO_4^{2-}})$$
$$= \frac{1}{2}(2b_{CH_3COO^-} + 6b_{SO_4^{2-}})$$
$$= b_{CH_3COO^-} + 3b_{SO_4^{2-}} \approx C_A\alpha + 3C_{SO_4^{2-}} \tag{19}$$

$K_{a,AcH}$ cannot be considered as a constant at high temperatures. It can be estimated from the following equation related by standard dissociation free energy of AA (ΔG^0) with its value of 27.2 kJ [18].

$$\ln K_a = \frac{-\Delta G^0}{RT} \tag{20}$$

Finally an expression for estimation of H^+ concentration was obtained as:

$$[H^+]$$
$$= \frac{2C_{SO^{2-}} + \sqrt{(2C_{SO^{2-}})^2 + 4(C_{A0} + C_{C0} - C_C)K_{C,AcH}}}{2} \tag{21}$$

and

$$K_{C,AcH} \approx \frac{\exp(-3271.59/T)}{\exp\left\{-2.342\left[\sqrt{[(C_{A0} + C_{C0} - C_C)\alpha + 3C_{SO_4^{2-}}]}/(1 + \sqrt{[(C_{A0} + C_{C0} - C_C)\alpha + 3C_{SO_4^{2-}}]})\right.\right.}$$
$$\left.\left. - 0.30[(C_{A0} + C_{C0} - C_C)\alpha + 3C_{SO_4^{2-}}]\right]\right\} \tag{22}$$

According to Eq. (20), the value of K_a at 353 K is 9.44×10^{-5}, which indicates that only about 0.2% of AA dissociates to CH_3COO^- and H^+ in the system when SA is absent. On the other hand, the dissociation of AA can be hindered by strong acid. Therefore, AA exits nearly as molecule form in the system, and H^+ can be thought only being from complete dissociation of SA.
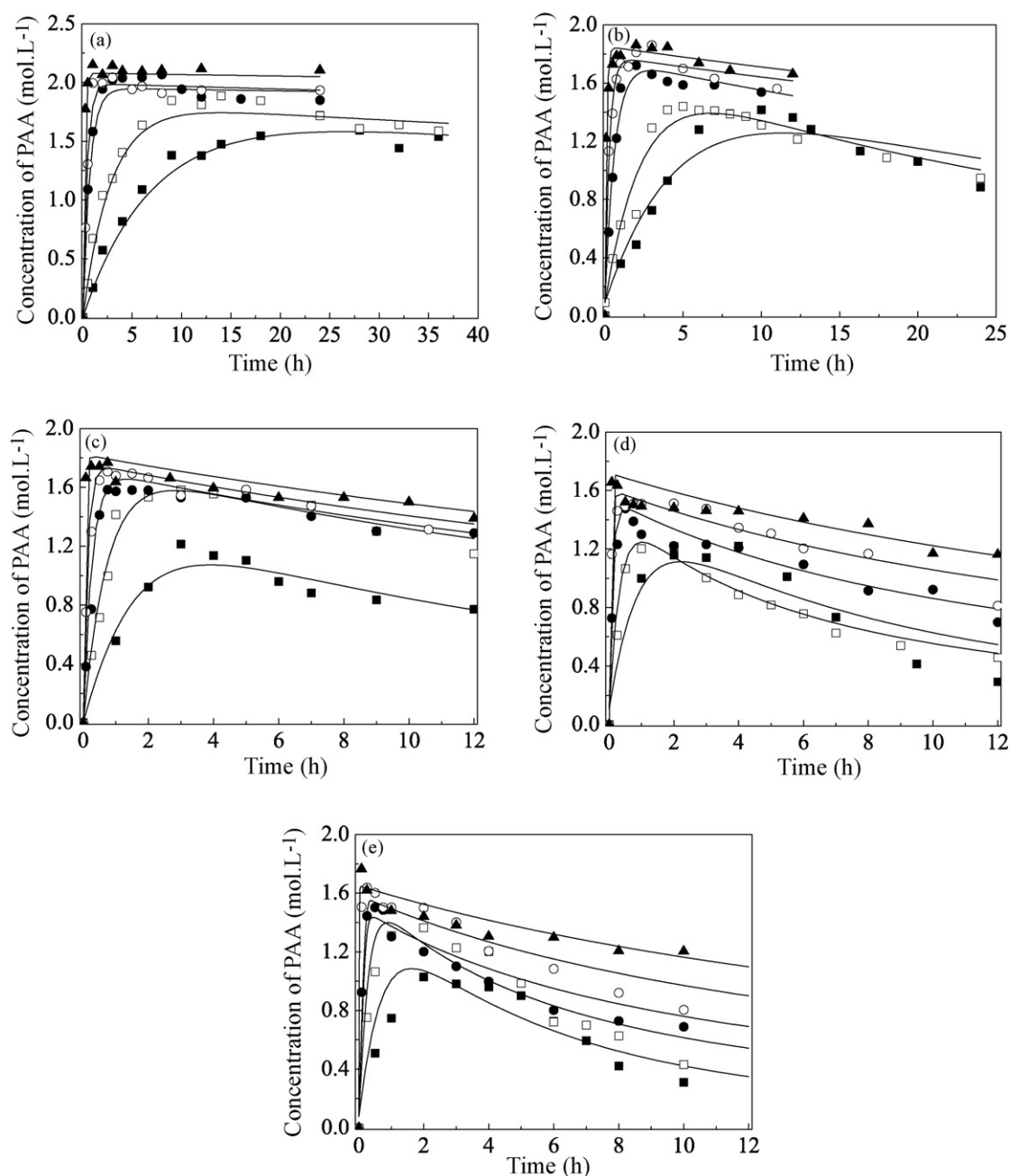
Fig. 3. Experimental and calculated concentrations of PAA at several temperatures with different charge of sulfuric acid as catalyst: (a) $T = 328$ K; (b) $T = 338$ K; (c) $T = 348$ K; (d) $T = 358$ K; (e) $T = 368$ K. (($\blacksquare$) 0.00 mol L^{-1} H$_2$SO$_4$; ($\square$) 0.0125 mol L^{-1} H$_2$SO$_4$; ($\bullet$) 0.0626 mol L^{-1} H$_2$SO$_4$; ($\bigcirc$) 0.1250 mol L^{-1} H$_2$SO$_4$; ($\blacktriangle$) 0.3125 mol L^{-1} H$_2$SO$_4$; ($\square$) calculated values).

3.3. Determination of kinetic constants

The experimental and model-calculated time profiles of PAA and HP concentration are shown in Figs. 3 and 4. The PAA concentration increased first and declined after a maximum, which was different from the time profiles at a temperature below 323 K. The HP concentration decreased steadily when temperature was above 338 K. It also can be seen that increasing temperature or decreasing charge of SA led to a more distinct decline of PAA and HP concentration. The figures showed that the model could well predict the trends of PAA and HP concentration. Tables 1–3 show the observed rate con-

stants determined by experimental data. It is clear that all the observed rate constants were increased with temperature at a fixed SA concentration. k_{1obs} and k_{2obs} were increased with SA concentration at a fixed temperature, but k_{3obs} was oppositely decreased when the charge of SA was increased. It showed that addition of SA could reduce the decomposition of PAA.

The plots of k_{1obs} versus [H$^+$] and k_{2obs} versus [H$^+$] shown in Fig. 5(a and b) indicated that both of k_{1obs} and k_{2obs} had linear relations with [H$^+$] at a temperature below 358 K, but the lines bended upward when temperature was over 358 K. It indicated that a high temperature led to a deviation of linear
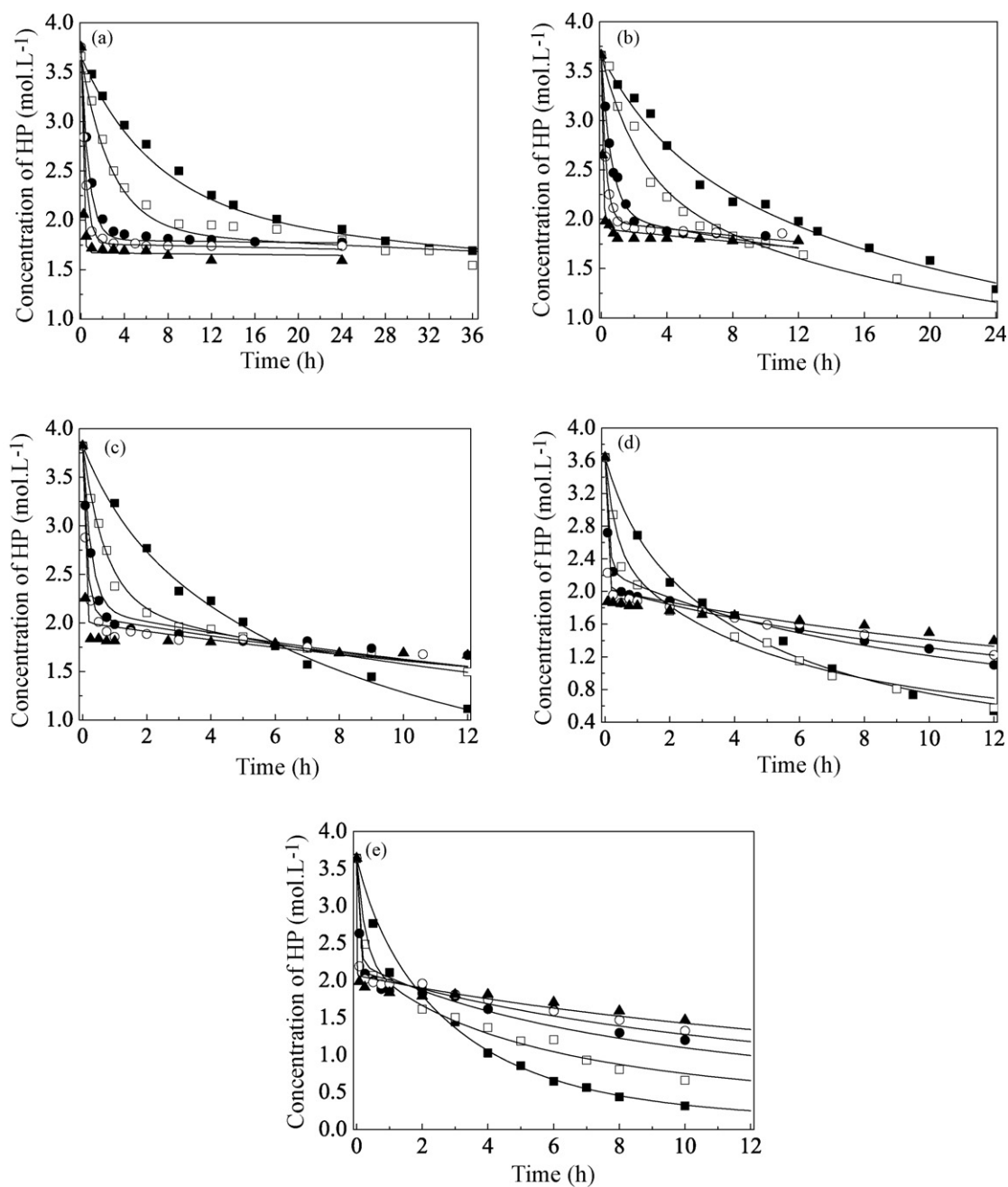
Fig. 4. Experimental and calculated concentrations of HP at several temperatures with different charge of sulfuric acid as catalyst: (a) $T = 328$ K; (b) $T = 338$ K; (c) $T = 348$ K; (d) $T = 358$ K; (e) $T = 368$ K. ((■) 0.00 mol L^{-1} H$_2$SO$_4$; (□) 0.0125 mol L^{-1} H$_2$SO$_4$; (●) 0.0626 mol L^{-1} H$_2$SO$_4$; (○) 0.1250 mol L^{-1} H$_2$SO$_4$; (▲) 0.3125 mol L^{-1} H$_2$SO$_4$; (—) calculated values).

Table 1
Values of k_{1obs} (L mol^{-1} h^{-1}) at different temperatures and different concentration of H$_2$SO$_4$

H$_2$SO$_4$ concentration (mol L^{-1})	T (K)				
	328	338	348	358	368
0	0.006322	0.006682	0.018966	0.035737	0.044704
0.0125	0.016883	0.017468	0.058602	0.109085	0.154649
0.0626	0.072538	0.072238	0.161988	0.371775	0.529013
0.1250	0.122800	0.162225	0.338150	0.831900	1.531500
0.3125	0.380125	0.507938	1.111375	2.614625	4.801813

Table 2
Values of k_{2obs} (L mol^{-1} h^{-1}) at different temperatures and different concentration of H_2SO_4

H_2SO_4 concentration (mol L^{-1})	T (K)				
	328	338	348	358	368
0	0.002837	0.002629	0.008159	0.014760	0.011493
0.0125	0.007555	0.008141	0.030626	0.070635	0.086345
0.0626	0.029088	0.036513	0.088675	0.246475	0.362900
0.1250	0.046975	0.080250	0.176900	0.481825	0.950600
0.3125	0.130125	0.231625	0.543438	1.447063	2.750750

Table 3
Values of k_{3obs} (L mol^{-1} h^{-1}) at different temperatures and different concentration of H_2SO_4

H_2SO_4 concentration (mol L^{-1})	T (K)				
	328	338	348	358	368
0	0.0057	0.0446	0.1968	0.3049	0.5093
0.0125	0.0033	0.0469	0.1063	0.3131	0.2488
0.0626	0.0017	0.0181	0.0383	0.1283	0.1648
0.1250	0.0012	0.0110	0.0329	0.0754	0.0957
0.3125	0.0006	0.0096	0.0269	0.0530	0.0586

relation between k_{1obs} or k_{2obs} and [H$^+$], which was probably because that high temperature enhanced the actual H$^+$ concentration in the liquid phase due to the evaporation of water and PAA. Therefore, the experimentally determined observed rate constants were increased. We have obtained the expressions for k_{1obs} or k_{2obs} in the temperature range of 293–323 K as:

$$k_{1obs} = k_1[H^+] = [H^+] \times 6.83 \times 10^8 \times \exp\left(-\frac{57846.15}{RT}\right)$$

(23)

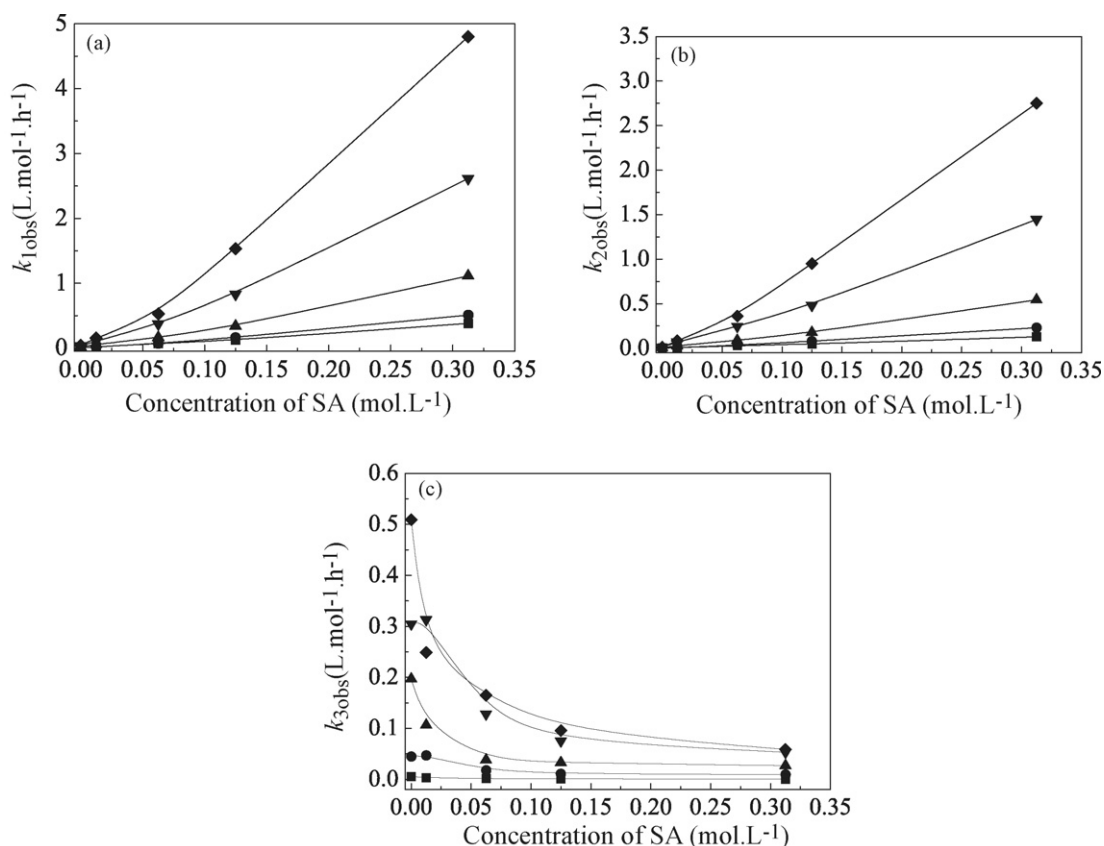Fig. 5. Plots of observed rate constants versus [H$^+$]; (a) k_{1obs} versus [H$^+$]; (b) k_{2obs} versus [H$^+$]; (c) k_{3obs} versus [H$^+$] ((■) 328 K; (●) 338 K; (▲) 348 K; (▼) 358 K; (♦) 368 K).
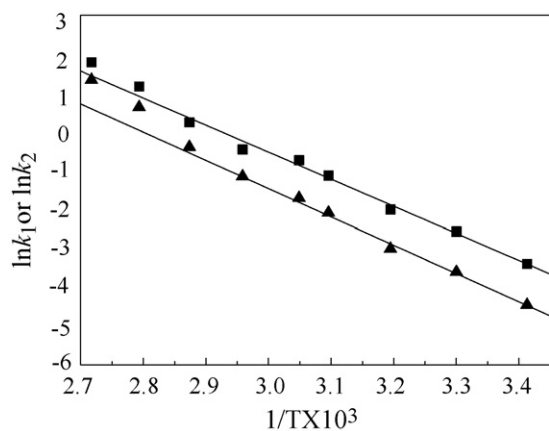
Fig. 6. Comparison of the experimentally determined data with the calculated data; (■) for k_1; (▲) for k_2; (—) calculated data.

$$k_{2obs} = k_2[H^+] = [H^+] \times 6.73 \times 10^8 \times \exp\left(-\frac{60407.78}{RT}\right)$$
(24)

where k_1 and k_2 are intrinsic rate constants for forward and reverse reactions, respectively [11]. We further compared the experimentally determined values for k_1 or k_2 with the calculated ones (Fig. 6). It can be seen that the models could well predict the experimental data except for some experimental points at a high temperature. Therefore, these expressions can be used for estimation of k_{1obs} or k_{2obs} at a temperature below 358 K with good accuracy.

Non-linear relation was observed between k_{3obs} and $[H^+]$, as shown in Fig. 5(c). It demonstrated that the spontaneous decomposition of PAA was not an acid-catalyzed process seemingly. The details will be discussed in next part of this work.

3.4. Reaction mechanism of spontaneous decomposition of PAA

3.4.1. Reaction steps

Koubek [12] and Yuan et al. [13] proposed the reaction mechanism for spontaneous decomposition of PAA in the pH range of 5.9–10.2 as shown in Scheme 1 (see part 1). They claimed that peraetic anion played as a nucleophile and the electrophilic site was carbonyl carbon rather than peroxidic oxygen. Some other studies of the spontaneous decomposition of various peracids showed that the rate of disappearance of the total peracid (RCOOH) was first-order with respect to the concentration of peracid anion (ROO−), and the decomposition rate reached its maximum when pH was equal to the pK_a of the peracid [19–22]. Therefore, peracid anion is an important species inducing the spontaneous decomposition of peracids under a neutral or alkaline condition. However, this scheme was not appropriate for our system. On the other hand, few published papers refer the reaction mechanism of PAA spontaneous decomposition in an acid system. The aim of this part is to make a discussion on the reaction mechanism.
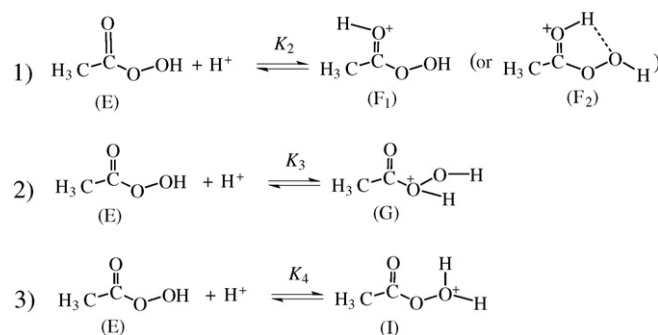
Scheme 2. Proposed reaction mechanism—step 1: protonation of oxygen atoms in PAA molecule.
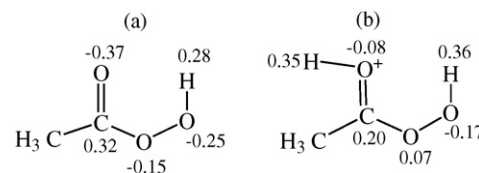

Scheme 3. Distribution of charges in PAA molecule (a) and protonated PAA molecule (b).

From Fig. 5(c) we can see that SA had a positive effect on reduction of PAA decomposition, which indicated that H+ took part in the reaction. However, the non-linear decrease of k_{3obs} demonstrated that the process was not a simple acid-catalyzed process. We suppose that the reaction mainly consists of three steps: protonation of the oxygen atom, formation of intermediary and formation of the final products.

The first step is the protonation of the oxygen atom in PAA molecule. There are three oxygen atoms in PAA molecule and each of them has certain negative charge. Therefore, three isomers (denoted as F_1/F_2, G and I, respectively) can be formed by protonation of corresponding oxygen atom, as shown in Scheme 2.

Thereinto, "E" denotes the PAA molecule and K_2 to K_4 denote corresponding equilibrium constants. According to Shi et al. [23], the first way is the most probable because that there is the richest negative charge on the carbonyl oxygen atom, as shown in Scheme 3(a). On the other hand, the isomer F_1/F_2 can be stabilized by a resonance effect of electron to quickly form a more stable intermediary J (Scheme 4). The carbonyl carbon in isomer J is thus activated and much more electrophilic than those in E and F.

In the second step, the activated carbonyl carbon is attacked by a nucleophilic agent to form an active intermediary. After a protonation, the negative charge on the oxygen atoms is reduced [23], as shown in Scheme 3(b). Therefore, F or J is not likely to
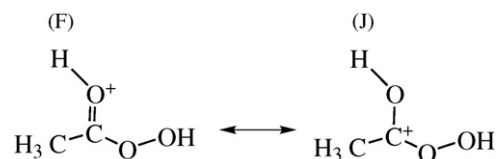
Scheme 4. Resonance effect of electron between isomer F_1/F_2 and J.
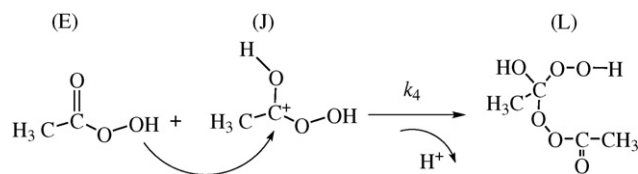
Scheme 5. Proposed reaction mechanism—step 2: formation of an active intermediary.

be a nucleophilic agent. The most probable pathway is that the oxygen atom of hydroxyl in PAA molecule attacks the activated carbonyl carbon followed by formation of an active intermediary L, as shown in Scheme 5.

In the last step, the unstable intermediary L quickly decomposes to AA and oxygen (see Scheme 6).

Another aspect should be noted is that HP also can play as a nucleophilic agent and attack isomer J. However, the p–π conjugate system in acetyl group of PAA molecule can make the hydroxyl oxygen atom attract more negative charge from hydrogen atom by an induction effect. Therefore, PAA molecule is more nucleophilic than HP molecule, and Scheme 5 is the most probable way.

3.4.2. The rate-determining step

The spontaneous decomposition of PAA is an observed second-order reaction with respect to PAA concentration. In order to determine which step is the rate-determining one, we employ a pre-equilibrium postulation for the first step, which means that the protonation reactions can reach equilibrium very quickly. Therefore, the experimentally determined concentration of PAA, C_C, can be expressed as:

$$C_C = C_E + C_J + C_G + C_I \tag{25}$$

where C_E is the concentration of PAA molecule; C_J, C_G and C_I are corresponding concentration of isomer J, G and I. They also can be related by corresponding equilibrium constant K_2, K_3 and K_4, as follows: $C_J = K_2 C_E[H^+]$, $C_G = K_3 C_E[H^+]$ and $C_I = K_4 C_E[H^+]$. Therefore, C_C and C_E can be expressed as:

$$C_E = \frac{C_C}{1 + (K_2 + K_3 + K_4)[H^+]} \tag{26}$$

Since the most probable way of protonation is the first one, namely $K_2 \gg K_3, K_4$, Eq. (26) can be simplified as:

$$C_E \approx \frac{C_C}{1 + K_2[H^+]} \tag{27}$$

The second step is a reaction of two large molecules, so we suppose it a rate-determining step. The third step is also very fast, namely $k_5 \gg k_4$. Therefore, the rate of consumption of PAA by
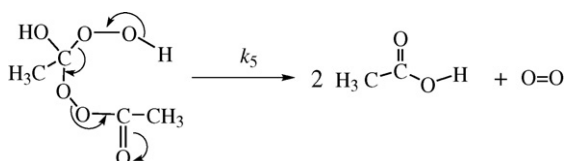
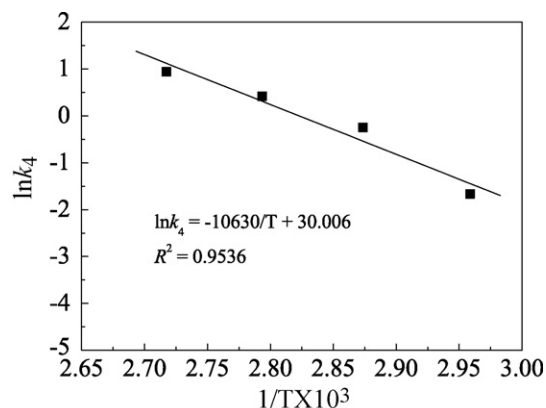Scheme 6. Proposed reaction mechanism—step 3: formation of final products.

Fig. 7. Relation of k_4 and T.

spontaneous decomposition can be written as:

$$-\left.\frac{dC_C}{dt}\right|_{\text{decompositon}} \approx k_4 C_E C_J = k_4 K_2[H^+]C_E^2$$

$$= \frac{k_4 K_2[H^+]}{(1 + K_2[H^+])^2}C_C^2$$

$$= k_{3\text{obs}} C_C^2 \tag{28}$$

The above differential equation is in accordance with our initial observed kinetic equation of spontaneous decomposition of PAA, which indicates that the presumed scheme is a feasible reaction mechanism for PAA decomposition under an acid condition. Eq. (28) also gives the relation between $k_{3\text{obs}}$ and $[H^+]$ as:

$$k_{3\text{obs}} = \frac{k_4 K_2[H^+]}{(1 + K_2[H^+])^2} \tag{29}$$

Both of them are functions of temperature. The experimentally determined relation of k_4 and T is shown in Fig. 7 and expression (30), and those of K_2 and T are shown in Fig. 8 and Eq. (31), respectively.

$$k_4 = 1.075 \times 10^{13} \exp\left(-\frac{88377.82}{RT}\right) \tag{30}$$
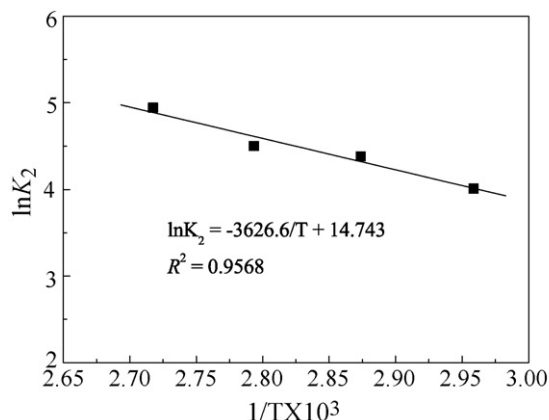

Fig. 8. Relation of K_2 and T.

Table 4
Comparison of the calculated equilibrium concentration (C_{Ce} (cal.)) of PAA by our model with corresponding experimental values (C_{Ce} (exp.)) from some references

Strength of HP used (%, w/w)	Molar ratio of AA/HP	C_{Ce} (exp.) (mol L^{-1})	C_{Ce} (cal.) (mol L^{-1})	δ^a (%)
27	4.05	1.82[b]	1.83	0.51
27	1.35	1.63[b]	1.76	7.99
50	1.01	1.63[c]	1.59	2.38
50	2.00	3.27[c]	3.56	8.66
50	4.00	2.64[c]	2.71	2.49
50	6.66	1.95[c]	1.95	0.11
50	10.00	1.42[c]	1.43	1.16
64.8	1.25	5.13[d]	4.81	−6.24
90	1.50	6.52[d]	6.27	−3.91

[a] The difference of calculated value and experimental value defined as: $\delta = [C_{Ce}$ (cal.) $- C_{Ce}$ (exp.)]$/C_{Ce}$ (exp.) $\times 100\%$.
[b] Data from Yang et al. [24].
[c] Data from John and Weymouth [10].
[d] Data determined in our experiment at 303 K. The average density of liquid mixture was calculated by the following expression: $\rho_m = 1/\sum_i x_i/\rho_i$, where x_i and ρ_i are the weight fraction and density of species i, respectively.

$$K_2 = 2.528 \times 10^6 \exp\left(-\frac{30151.55}{RT}\right) \tag{31}$$

Therefore, we obtained an expression for k_{3obs} as:

$$k_{3obs} = \frac{2.72 \times 10^{19} \exp(-118529.37/RT)[\text{H}^+]}{\{1 + 2.528 \times 10^6 \exp(-30151.55/RT)[\text{H}^+]\}^2} \tag{32}$$

Corresponding PAA and HP concentration during preparation can be estimated according to the following equations:

$$\frac{dC_{PAA}}{dt} = 6.83 \times 10^8 \times \exp\left(-\frac{57846.15}{RT}\right)[\text{H}^+]C_{AA}C_{HP}$$
$$- 6.73 \times 10^8 \times \exp\left(-\frac{60407.78}{RT}\right)[\text{H}^+]C_{PAA}C_{H_2O}$$
$$\times \frac{-2.72 \times 10^{19} \exp\left(-\frac{118529.37}{RT}\right)[\text{H}^+]}{\{1 + 2.528 \times 10^6 \exp\left(-\frac{30151.55}{RT}\right)[\text{H}^+]\}^2}C_{PAA}^2 \tag{33}$$

$$\frac{dC_{HP}}{dt} = 6.73 \times 10^8 \times \exp\left(-\frac{60407.78}{RT}\right)[\text{H}^+]C_{PAA}C_{H_2O}$$
$$- 6.83 \times 10^8 \times \exp\left(-\frac{57846.15}{RT}\right)[\text{H}^+]C_{AA}C_{HP} \tag{34}$$

3.5. Application of the kinetic model

From Tables 2 and 3, it can be known that the ratio of k_{2obs}/k_{3obs} at 328 K was 17–217 when SA concentration was in the range of 0.0626–0.3125 mol L^{-1}. It shows that the spontaneous decomposition of PAA with presence of SA at a temperature below 328 K becomes so insignificant that can be negligible. On the other hand, there is always large amount of water in the system and the hydrolysis of PAA is the predominant consumption pathway for PAA. Therefore, at a low temperature the system mainly consists of the reversible reaction as shown

in Eq. (9). The equilibrium constant for this reversible reaction obtained from Eqs. (23) and (24) was:

$$K_C = \frac{k_1}{k_2} = 1.015 \times \exp\left(\frac{2561.63}{RT}\right) \tag{35}$$

Based on this expression, we can estimate the equilibrium constant and thus predict the equilibrium concentration of PAA by the following expression:

$$C_{Ce} = \frac{K_C C_{A0} + K_C C_{B0} + C_{D0}}{2(K_C - 1)}$$
$$- \frac{\sqrt{(K_C C_{A0} + K_C C_{B0} + C_{D0})^2 - 4K_C C_{A0} C_{B0}(K_C - 1)}}{2(K_C - 1)} \tag{36}$$

where C_{Ce} is the equilibrium concentration of PAA. We compared the calculated values of C_{Ce} based on expression (35) and (36) with the experimental values from some references, as shown in Table 4. It was found that our model could predict the values of PAA concentration with sufficient accuracy.

On the other hand, the standard Gibbs energy change of molar reaction for the forward reaction, $\Delta_r G_m^0$, estimated according to Eq. (35) was -2.56 kJ mol^{-1} approximately. The standard molar formation Gibbs energy of PAA, $\Delta_f G_m^0|_{PAA}$, calculated based on Eq. (37) was -276 kJ mol^{-1} approximately. These data can be used for some other related studies, since they are not available from the handbook.

$$\Delta_r G_m^0 = \sum \Delta_f G_m^0|_X \tag{37}$$

4. Conclusions

The kinetics for spontaneous decomposition of PAA in the liquid phase under an acid condition in the temperature range of 328–368 K was developed, with the kinetic constants being determined according to the experimental data. It was found that the chelant DTPA was not so effective for reduction of PAA decomposition in a strong acid solution as it in a neutral or alkaline aqueous solution. The spontaneous decomposition

of PAA under an acid condition was an observed second-order reaction with respect to PAA concentration and the observed rate constant was a relatively complicated function of temperature and H^+ concentration. Addition of SA could obviously decrease the spontaneous decomposition of PAA. The model described that the spontaneous decomposition of PAA at a temperature below 328 K was so insignificant that could be negligible and hydrolysis became the predominant consumption for PAA. It was proved that the rate-determining step for the spontaneous decomposition of PAA was the reaction between PAA molecule and a proton-activated carbonyl intermediary.

Acknowledgment

References

[1] L.B. Brasileiro, J.L. Colodette, D. Pilo-Veloso, Quim. Nova. 24 (2001) 819–829.
[2] R. Gehr, M. Wagner, P. Veerasubramanian, P. Payment, Water Res. 37 (2003) 4573–4586.
[3] M. Kitis, Environ. Int. 30 (2004) 47–55.
[4] Y. Cai, S.K. David, Text. Res. J. 67 (1997) 459–464.
[5] Z. Yuan, Y. Ni, A.R.P. Van Heiningen, Appita J. 51 (1998) 377–380.
[6] Q. Yang, F. Tang, Y. Zhang, China Pulp Pap. 22 (2003) 5–8.
[7] P. Krizman, F. Kovac, F.T. Petra, Color. Technol. 121 (2005) 304–309.
[8] D.H. Stormont, Oil Gas J. 58 (1960) 78–79.
[9] R.L. Musante, R.J. Grau, M.A. Baltanas, Appl. Catal. A: Gen. 197 (2000) 165–173.
[10] J.A. John, F.J. Weymouth, Chem. Ind. 2 (1962) 62–69.
[11] X.B. Zhao, T. Zhang, Y.J. Zhou, D.H. Liu, J. Mol. Catal. A-Chem. 271 (2007) 246–252.
[12] E. Koubek, The kinetics and the mechanism of the decomposition of aliphatic peroxyacids in aqueous solutions, Ph.D thesis, Brown University, New York, 1964.
[13] Z. Yuan, Y. Ni, A.R.P. Van Heiningen, Can. J. Chem. Eng. 75 (1997) 37–41.
[14] Z. Yuan, Y. Ni, A.R.P. Van Heiningen, Can. J. Chem. Eng. 75 (1997) 42–47.
[15] E. Koubek, M.L. Haggett, C.J. Battaglia, K.M. Ibne-Rasa, H.Y. Pyun, J.O. Edwards, J. Am. Chem. Soc. 85 (1963) 2263–2268.
[16] Z. Yuan, M. d'Entremont, Y. Ni, A.R.P. van Heiningen, J. Wood Chem. Technol. 18 (1998) 267–288.
[17] J.F. Kadla, H. Chang, ACS Sym. Ser. 785 (2001) 108–129.
[18] H. Shen, Organic Acid and Base, Higher Education Press, Beijing, 1983, pp. 78–79.
[19] L.D. Ball, J.O. Edwards, J. Am. Chem. Soc. 78 (1956) 1125–1129.
[20] R.E. Ball, J.O. Edwards, M.L. Haggett, P. Jones, J. Am. Chem. Soc. 89 (1967) 2331–2333.
[21] J.F. Goodman, P. Robson, Trans. Faraday Soc. 59 (1963) 2871–2875.
[22] R.C. Francis, X.Z. Zhang, P.M. Froass, O. Tamer, Tappi J. 77 (1994) 133–140.
[23] H. Shi, Z. Zhang, Y. Wang, J. Mol. Catal. A-Chem. 238 (2005) 13–25.
[24] H.S. Yang, Y. Lu, Q.H. Meng, S. Zhang, G.H. Zhang, J. Qinghai Univ. 22 (2004) 68–70.